

⁷The zero on the φ scale corresponds to the [110] direction lying on the diffraction plane.

⁸P. B. Hirsch and G. N. Ramachandran, *Acta Crystallogr.* **3**, 187 (1950).

⁹In electron diffraction, "virtual Bragg scattering" is a common occurrence and must be always taken into

account in quantitative experiments. See, for example, F. Fujimoto, *J. Phys. Soc. Jpn.* **15**, 1022 (1960), on the (222) reflection in silicon.

¹⁰The need of using a dynamical N -beam diffraction theory for imperfect crystals was pointed out by M. Kuriyama, *Acta Crystallogr. Sect. A* **25**, 56 (1969).

Domain Growth of Degenerate Phases

S. A. Safran

Theoretical Sciences Group, Exxon Research and Engineering, Linden, New Jersey 07036
(Received 12 March 1981)

The domain-coarsening kinetics of ordering systems with p -fold-degenerate equilibrium states, quenched from high temperatures, is analyzed. For long times (t) and low temperatures, the domain sizes equilibrate as a power law in t for $p < d + 1$ and as a logarithmic function of t for $p \geq d + 1$, where d is the spatial dimensionality of the system. The relation of these slowly equilibrating, kinetically disordered systems to glasses and suggestions for simulations and experiments are discussed.

PACS numbers: 64.60.My, 05.70.Fh, 81.30.Fb

The structures of charge-density-wave systems,¹ adsorbed atoms on surfaces,² some intercalation compounds,³ ordering alloys,^{4,5} and antiferromagnets^{6,7} are all characterized by a discrete number of low-temperature phases which are thermodynamically degenerate. For example, certain ordered phases of rare-gas atoms on the surface of Grafoil consist of three equivalent sublattices (degeneracy $p = 3$), whose thermodynamics is derived from a Hamiltonian of the three-state Potts model.² Recent Monte Carlo calculations of the approach to equilibrium of ordering alloys and magnets quenched from high temperatures have indicated that, for spatial dimensionality $d = 3$, systems with twofold-degenerate low-temperature equilibrium phases ($p = 2$) do approach equilibrium as expected, with large domains of equivalent phases.⁸ However, the four-state antiferromagnetic Potts model⁷ in $d = 3$, as well as^{3,9} the three-state ferromagnetic Potts model ($p = 3$) for $d = 2$, has been reported⁷⁻⁹ to maintain some of their quenched-in disorder for quenches from high to low temperatures. This phenomenon is reminiscent of descriptions of glasses¹⁰ and is in agreement with a discussion by Lifshitz¹¹ of the difficulty of equilibrating systems with $p \geq d + 1$.

This paper is a first step in establishing a quantitative basis for this suggestion by Lifshitz,¹¹ using a time-dependent Ginzburg-Landau approach^{12,13} to calculate the domain-growth rate for various values of d and p . The equilibration

of systems with $p \geq d + 1$ is shown to be frustrated and hence characterized by a domain size which grows only logarithmically in time. While some of the arguments given here are independent of the details of any particular system, it is useful to consider a specific model. For example, the three-state Potts model¹⁴ represents a system where each lattice site is characterized by a spin which can have three possible values. The order parameter consists of an amplitude ρ and a phase η .¹⁴ For fixed ρ , the free energy is minimized by uniform, degenerate phases with $\eta = 0$ and $\pm \frac{2}{3}\pi$ representing the three possible spin values. For long times after a quench from a high-temperature (T) disordered phase ($\rho = 0$), it is expected that the system is uniformly characterized by its equilibrium value of $\rho_0(T)$ and by a spatially non-uniform $\eta(\vec{r})$, describing the arrangement of microdomains whose characteristic size is much greater than that of a lattice constant, but much smaller than that of the sample.¹⁵

For uniform $\rho = \rho_0(T)$, the free-energy density $F(\vec{r})$ can be written¹⁴ in a continuum approximation as

$$F = F_0 - \frac{1}{3}b \cos 3\eta \rho_0^3 + \frac{1}{2}c\rho_0^2 |\nabla\eta|^2, \quad (1)$$

where b and d are positive constants and where F_0 is the free energy of the uniform, single-domain system. Rescaling the energy by $b\rho_0^3$, the length by $(c/b\rho_0)^{1/2}$, and generalizing to p -fold-degenerate systems, the time dependence of η is

related to the excess free-energy density $f(\vec{r}) = [F(\vec{r}) - F_0(\vec{r})]/b\rho_0^3$ by^{12,13}

$$\partial\eta/\partial t = -\Gamma \delta f/\delta\eta = -\Gamma(-\nabla^2\eta + \partial V/\partial\eta), \quad (2)$$

where Γ is a constant and $V(\eta) = \frac{1}{3}[1 - \cos(p\eta)]$.

After the initial equilibration of ρ , the system consists of domains of $\eta \approx 0, 2\pi/p, \dots, 2\pi(p-1)/p$. In any given region, equilibrium is reached by the shrinking of some domains and a consequent growth of others. The coarsening process is analyzed here by examining the time evolution of a single domain of one value of η , surrounded by an infinite matrix of domains of the other $p-1$ values of η (Figs. 1-4). The angles between the domain walls are assumed [this is demonstrated in (iii) below] to have reached their equilibrium values at the late times of interest here. The approach to equilibrium is then analyzed by calculations of the growth or shrinking of the domain size L .

In the limit of highly localized domain walls, it can be argued from Figs. 1(a) and 1(b) that for $d=1$ and $p \geq 2$, there is no change in the free energy when L is infinitesimally changed ($L=L_0 + \Delta L$) since two walls still exist. On the other hand, for $p=2$ and $d=2$ or $d=3$, the change in the free energy is proportional to L_0^{d-1} which provides a driving force for the shrinking of the minority domain. For $d=2$ and $p=3$, the shrinking of domain A in Fig. 4 results in a reduction of the perimeter of the domain A by $6\Delta L$. However, at the same time, the walls separating domains B and C increase in length by $6\Delta L$, thus preventing the system from either shrinking or growing the A phase and proceeding to equilibrium. Similar arguments,¹⁵ applied to $d=3$, show that structures with $p \leq 3$ reduce the net domain-wall area by shrinking the minority domain, while

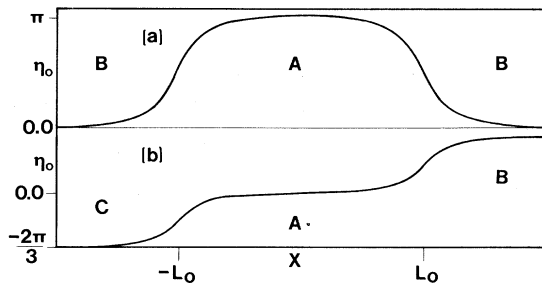


FIG. 1. One-dimensional domains (calculated for $L_0 = 5$). (a) $p = 2$; a domain (A) of $\eta_0 \approx \pi$ surrounded by domains (B) of $\eta_0 \approx 0$. (b) $p = 3$; a domain (A) of $\eta_0 \approx 0$ surrounded by domain (B) of $\eta_0 \approx \frac{2}{3}\pi$ and a domain (C) of $\eta_0 \approx -\frac{2}{3}\pi$.

systems with $p > 4$ show no change in energy for small changes in L .

To see the effects of the delocalization of the domain walls and to calculate the time dependence of the shrinking/coarsening process, Eq. (2) is used. If at time $t=0$ the domain configuration is given by $\eta = \eta_0(\vec{r})$, then a short time Δt later, $\eta = \eta_0 + \Delta\eta$, where

$$\Delta\eta \approx -\Gamma \Delta t (\partial V/\partial\eta_0 - \nabla^2\eta_0). \quad (3)$$

In the following, $\Delta\eta$ and $L(t)$ are calculated explicitly for several cases (values of p and d), in the approximation¹⁶ that $V(\eta)$ in Eq. (2) is given by a periodic, truncated parabola

$$V(\eta) = \frac{1}{2}\eta^2, \quad -\pi/p \leq \eta \leq \pi/p, \quad (4a)$$

$$V(\eta + 2\pi/p) = V(\eta). \quad (4b)$$

(i) $d=1$; $p=2, 3$: The $t=0$ configuration shown in Fig. 1(a) is obtained from the time-independent solution of Eq. (2) for a potential $V(\eta)$ similar to that of Eq. (4), but with a term which breaks the symmetry between the degenerate phases,¹⁵ so that

$$\eta_0 = \frac{1}{2}\pi \exp[-(x - L_0)], \quad x \geq L_0, \quad (5a)$$

$$\eta_0 = \pi - \frac{1}{2}\pi \cosh\gamma x / \cosh\gamma L_0, \quad 0 \leq x \leq L_0, \quad (5b)$$

where η_0 is symmetric about $x=0$ and $\gamma \tanh\gamma L_0 = 1$. For large L_0 , the free energy is lower than the free energy for $L_0 \rightarrow \infty$ by a term proportional to $\exp(-2L_0)$, representing an attractive interaction between the two domain walls. A short time Δt later, Eq. (3) [with the true degenerate potential of Eq. (4)] indicates that, for $x < L_0$,

$$\eta(x, \Delta t) \approx \eta_0(x)|_{L_0 \rightarrow L_0 + \Delta L}, \quad (6)$$

where $\Delta L \approx -4\Gamma \Delta t \exp(-2L_0)$. Letting $\eta(x, t)$ evolve in this manner, it is found that the effective length of the minority domain shrinks as

$$L = L_0 + \frac{1}{2} \ln[1 - 8\Gamma \exp(-2L_0)t]. \quad (7)$$

For the configuration of Fig. 1(b) ($d=1$ and $p=3$), a similar analysis shows that the minority do-

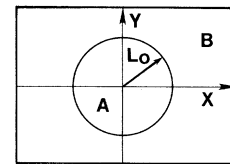


FIG. 2. Two-dimensional domains for $p = 2$ showing the locus of $\eta_0 = \frac{1}{2}\pi$ separating the ($\eta_0 \approx 0$) region A from the ($\eta_0 \approx \pi$) region B.

main *grows* as in Eq. (7) but with $\Gamma \rightarrow -\Gamma$. This corresponds to a repulsive interaction between the domain walls.

(ii) $d=2, 3; p=2$: For the configuration of Fig. 2, η_0 is calculated as in (i) and for $d=2$,

$$\eta_0 = \frac{1}{2}\pi I_0(\gamma r)/I_0(\gamma L_0), \quad r \leq L_0, \quad (8a)$$

$$\eta_0 = \pi - \frac{1}{2}\pi K_0(r)/K_0(L_0), \quad r \geq L_0, \quad (8b)$$

where I_0 and K_0 are the Bessel functions of imaginary arguments and $\gamma \approx 1 + 1/L_0$. Near the wall ($r \approx L$), Eq. (6) again applies but with $\Delta L \approx -4\Gamma \Delta t/L_0$ and for both $d=2$ and $d=3$ $L(t) = [L_0^2 - 2\Gamma t(d-1)]^{1/2}$.^{4,11,15}

(iii) $d=2; p=4$: Although the configuration shown by the solid lines in Fig. 3 is metastable—i.e., $\delta F/\delta \eta = 0$ —it is useful to study the response of this configuration to perturbations, in order to determine the nature of the interactions between the domain walls.

For the model potential [Eq. (4)] with $d=2$, a solution of $\delta F/\delta \eta = 0$ which describes four infinite domains with $\bar{\eta} \approx 0, \frac{1}{2}\pi, \pi$, and $\frac{3}{2}\pi$ is given for $x > 0, y > 0$, by

$$\bar{\eta} = \frac{1}{2} \int_0^\infty dk k^{-1} [\sin(kx)e^{-k'y} - \sin(ky)e^{-k'x}], \quad (9)$$

where $k'^2 = 1 + k^2$, with similar expressions for η in the other three quadrants. For an initial *unstable* configuration $\eta_0(x, y) = \bar{\eta}(x - \epsilon y, y)$ shown by the dashed line in Fig. 3, Eq. (3) indicates that for short times and to first order in ϵ , $\Delta \eta \approx \pm \epsilon \Delta t (\pi/2u)^{1/2} e^{-u}$, where $u = y$ and the positive sign applies for $x - \epsilon y = 0$, and $u = x - \epsilon y$ and the negative sign applies for $y = 0$. This corresponds to an exponential repulsion between the walls. For $x, y \ll 1$, a similar analysis shows that there is an even stronger repulsion between the walls with $\Delta \eta$ proportional to x^{-2} (y^{-2}) along the lines $y = 0$ ($x - \epsilon y = 0$),¹⁷ tending to fix the angles between the walls at $\frac{1}{2}\pi$ as claimed above.

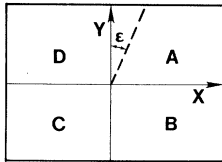


FIG. 3. Domains for $d=2$ and $p=4$. The solid line is the metastable wall configuration, where the line between domains A and B is $\eta = \frac{1}{4}\pi$, the line separating domains B and C is $\eta = \frac{3}{4}\pi$, the line between domains C and D is $\eta = \frac{5}{4}\pi$, etc. The dashed line represents the initial wall configuration ($\eta_0 = -\frac{1}{4}\pi$) discussed in the text.

(iv) $d=2; p=3$: For the configuration of Fig. 4, the previous analysis suggests that there exists an exponential repulsive interaction between any given wall (A, B) or (A, C) and its nearest neighbors [see (i)]. That this interaction persists for walls at angles to each other was demonstrated in (iii). The weak repulsion between walls (A, B) and (B, C) as well as the weak attraction between walls (A, B) both tend to shrink domain A with a logarithmically slow equilibration as discussed above [Eq. (7)].¹⁵

Although more quantitative calculations of $L(t)$ for $p > 2$ and $d > 2$ are clearly needed, the present work predicts a slow, logarithmic equilibration of the domains for $p \geq d+1$. For a system with an initial distribution of domain sizes and arrangements, this results in an effective freezing-in of the late time (ρ equilibrated) structure. These systems are thus simple examples of the formation of an amorphous or glassy structure due to the slow growth of domains, which are prevented from equilibrating by the other degrees of freedom in the system,¹⁸ in qualitative agreement with the Monte Carlo results.⁶⁻⁹

Recent simulations of the four-state antiferromagnetic Potts model for $d=3$ have resulted in glass formation for quenches from high ($T \gg T_c$) to low ($T \ll T_c$) temperatures, where T_c is the critical temperature.⁷ On the other hand, equilibrium *was* attained for quenches to temperatures exceeding about $\frac{1}{4}T_c$, suggesting the existence of a glass transition temperature (T^*). In the present work, the only temperature dependence lies in the scaling of the lengths by the temperature-dependent factor $(c/d\rho_0)^{1/2}$. Since $\rho_0(T)$ decreases as the temperature increases, this results in a larger coefficient of the time t in Eq. (7). However, extensions of these calculations

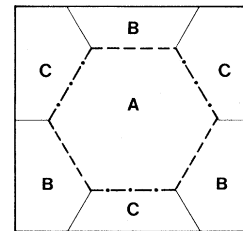


FIG. 4. Domains for $d=2$ and $p=3$. The solid line is the wall $\eta_0 = \pi$ separating the domains B and C with $\eta_0 \approx \frac{2}{3}\pi$ and $\eta_0 \approx -\frac{2}{3}\pi$, respectively. The dashed line is the locus of $\eta_0 = \frac{1}{3}\pi$ separating domain A with $\eta_0 \approx 0$ from domain B , while the dot-dashed line is $\eta_0 = -\frac{1}{3}\pi$ separating regions A and C .

are necessary to determine whether it is the simple length scaling, thermal fluctuations, or the simultaneous equilibration of both the amplitude and the phase of the order parameter that is responsible for the qualitatively different kinetics for $T > T^*$. Furthermore, it is not yet clear whether the simple free energy of Eq. (1), applicable to the ferromagnetic Potts model,^{2,8,9} can also be used to analyze the dynamics of the antiferromagnetic systems⁷ which have the complication of infinitely degenerate ground states.

The author wishes to thank J. S. Langer, R. W. Cohen, D. Gutkowitz, J. Chalupa, P. Sahni, J. Banavar, and J. R. Schrieffer for stimulating discussions.

¹D. E. Moncton, J. D. Axe, and F. J. DiSalvo, Phys. Rev. B **16**, 801 (1977).

²A. N. Berker, S. Ostlund, and F. A. Putnam, Phys. Rev. B **17**, 3650 (1978).

³N. Kambe, M. S. Dresselhaus, G. Dresselhaus, S. Basu, A. R. McGhie, and J. E. Fischer, Mater. Sci. Eng. **40**, 1 (1979).

⁴S. M. Allen and J. W. Cahn, Acta Metall. **27**, 1085

(1979).

⁵A. T. English, Trans. Metall. Soc. AIME **236**, 14 (1966).

⁶M. K. Phani, L. L. Lebowitz, M. H. Kalos, and O. Penrose, Phys. Rev. Lett. **45**, 366 (1980).

⁷J. R. Banavar, G. S. Grest, and D. Jasnow, Phys. Rev. Lett. **45**, 1424 (1980).

⁸J. Chalupa, unpublished.

⁹P. Sahni and J. Gunton, unpublished.

¹⁰R. O. Davies and G. O. Jones, Adv. Phys. **2**, 370 (1953).

¹¹I. M. Lifshitz, Zh. Eksp. Teor. Fiz. **42**, 1354 (1962) [Sov. Phys. JETP **15**, 939 (1962)].

¹²P. C. Hohenberg and B. I. Halperin, Rev. Mod. Phys. **49**, 435 (1977).

¹³J. S. Langer, Ann. Phys. (N.Y.) **65**, 53 (1971).

¹⁴S. Alexander, Solid State Commun. **14**, 1069 (1974).

¹⁵S. A. Safran, unpublished. This reference includes a discussion of thermal fluctuation effects neglected in the present work, which treats domain growth at low temperatures.

¹⁶P. Bak, in *Solitons and Condensed Matter Physics*, edited by A. T. Bishop and T. Schneider (Springer-Verlag, New York, 1978), p. 216.

¹⁷In a real, physical system, the singularity at the origin is removed by a vanishing amplitude at that point.

¹⁸J. C. Phillips, J. Non-Cryst. Solids **34**, 153 (1979).

Adsorbate-Induced Contracted Domain Structure: Nitrogen Chemisorbed on W{001}

Keith Griffiths, Christopher Kendon, and David A. King

The Donnan Laboratories, The University, Liverpool L69 3BX, United Kingdom

and

John B. Pendry

Science Research Council, Daresbury Laboratory, Daresbury, Warrington WA4 4AD, United Kingdom

(Received 18 February 1981)

A low-symmetry low-energy-electron-diffraction pattern observed at a fractional nitrogen-atom coverage of 0.4 monolayer on W{001} is attributed to a structure composed of islands in which the surface-layer tungsten atoms are displaced to produce a contracted interatomic spacing. The model correlates well with other published data for this system.

PACS numbers: 68.20.+t, 61.14.Hg

Extensive studies of the clean^{1,2} and hydrogen-covered^{3,4} W{001} surface have revealed that the tungsten atoms in this surface readily undergo small static lateral displacements from their high-symmetry bulk positions. All previous studies of nitrogen chemisorbed on W{001} have been interpreted without regard to possible substrate-surface-atom displacement.⁵⁻⁷ Thus Adams and Germer⁵ (hereafter AG), in the most detailed

structural study of this system to date, concluded that nitrogen adatoms occupy alternate undistorted fourfold-symmetric hollow sites, and attributed the observed splitting of the half-order diffraction beams at intermediate coverages to changes in average island or domain size and shape, with antiphase boundaries between domains.

In the coverage range $0.3 \leq \theta \leq 0.4$, careful observation of the low-energy-electron-diffraction